Pattern Formation in Binary Fluids Confined between Rough, Chemically Heterogeneous Surfaces

R. Verberg,[1] C. M. Pooley,[1] J. M. Yeomans,[2] and Anna. C. Balazs[1]

[1]*Chemical and Petroleum Engineering Department, University of Pittsburgh, Pittsburgh, Pennsylvania 15261, USA*
[2]*The Rudolf Peierls Centre for Theoretical Physics, Oxford University, 1 Keble Road, Oxford OX1 3NP, United Kingdom*

(Received 22 July 2004; published 26 October 2004)

Using a mesoscale model for hydrodynamics, we simulate driven flow of *AB* binary fluids past surfaces that contain well-defined roughness or asperities. The geometry and wetting properties of the asperities are found to have a dramatic effect on the flow patterns. We isolate conditions where the *A* fluid forms vertical bands that bridge the asperities and an imposed shear (or pressure gradient) drives the system to form monodisperse droplets of *A* within the *B* fluid. The size of the droplets can be tailored by varying the morphology of the asperities. The surfaces needed to create this rich dynamical behavior are used as the stamps in microcontact printing; thus, the parameter space can readily be accessed experimentally, and the predictions suggest an efficient method for forming emulsions with well-controlled morphologies.

DOI: 10.1103/PhysRevLett.93.184501 PACS numbers: 47.54.+r

From optimizing the processing of polymeric materials to controlling blood flow in natural or synthetic channels, it is vital to understand the dynamic behavior of complex fluids in confined geometries. Developing such an understanding is complicated by the fact that in the systems of interest, the confining walls can display chemical or physical heterogeneities and the fluid usually contains multiple components. Furthermore, this multicomponent mixture is driven by an imposed flow (which transports the fluid through the processing chambers or the blood vessels). In such systems, the fluid-wall, fluid-fluid, and fluid-flow interactions can all affect the phase behavior and morphology of the confined mixture. While researchers have recently examined how chemical variations on the confining walls affect the flow patterns of driven complex fluids [1], there have been few studies on the effect of surface roughness on such systems. Using a computational model, we undertake the first study of a binary phase-separating fluid that is driven to flow past surfaces which contain well-defined roughness or asperities. We focus on binary, immiscible fluids since this is the simplest multicomponent mixture that can display distinct pattern formation in response to the presence of the asperities. As we show below, the relative size and shape of the asperities has a dramatic effect on the flow patterns, dictating whether or not the system reaches a steady-state morphology or displays periodic structure formation within the confined mixture. In the former case, the *AB* mixture forms monodisperse droplets of *A* within the *B* phase; such emulsions are crucial constituents in the pharmaceutical, food, and cosmetic industries [2]. What sets the proposed method apart from other techniques for creating these mixtures [2,3] is that the droplet size is controlled by the surface morphology and chemistry, which can be readily manipulated by standard microcontact printing methods. In fact, the necessary surfaces are the "stamps" in this process. Hence, the findings suggest a means of forming monodisperse droplets of a variety of chemical components and range of sizes through a relatively facile process.

Before discussing the methodology for modeling the confined fluids, we lay out the principles that control the novel behavior of the system. Initially, the *A*-like bands lie perpendicular to the walls and bridge the narrow gap between the square asperities [Fig. 1(a)]. The height of the gap is given by H, the width of the asperities (and bands) is W, and the distance between the asperities is G. Because of the imposed shear, the bands are stretched [Fig. 1(b)] and eventually break off when the contact between the bands and surfaces occurs only at points on the corners of the asperities [Fig. 1(c)]. Earlier detachment would involve forming additional A/B interfaces

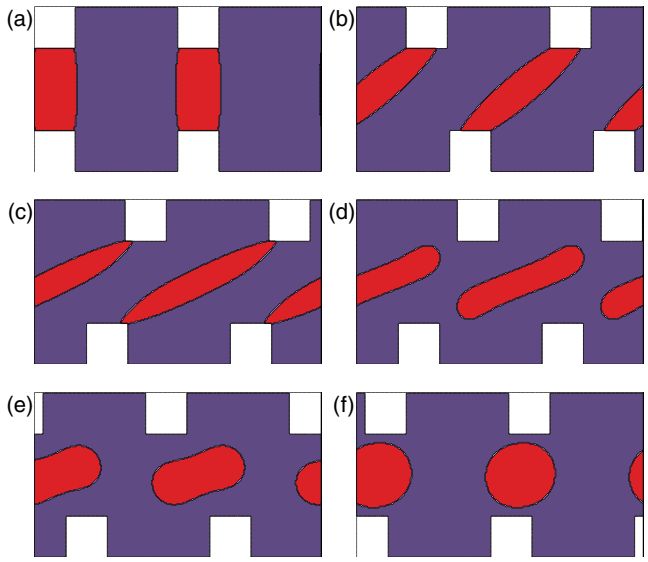

FIG. 1 (color online). Formation of droplets from a regular array of bands under shear.

 0031-9007/04/93(18)/184501(4)$22.50

near the surfaces and thus, is energetically unfavorable. After a short transient state [Fig. 1(d) and 1(e)], each band transforms into a single droplet in the center of the gap in order to minimize its surface area [Fig. 1(f)].

Figure 2 illustrates how the surface morphology and the ratio between the initial bandwidth, W, and gap height, H, affects this dynamical behavior. The figure shows snapshots of the system for three different ratios, $W/H = 1/4$, $1/2$, and 1, for square asperities that are separated by a distance equal to the bandwidth, i.e., $G = W$. Distinctly different behavior can be seen for the different ratios W/H. Below a critical ratio, the system evolves to a final steady state, with a single band of A in the center of the gap for $W/H = 1/4$ [Fig. 2(a)], or an array of A droplets for $W/H = 1/2$ [Fig. 2(b)]. Above the critical ratio, the bands break up and recombine in a periodic manner [Fig. 2(c)]. In the two-dimensional system studied here, this behavior can be qualitatively understood through simple arguments involving the interfacial length. These arguments are formulated for neutral wetting conditions on the asperities; i.e., the free energy contribution from the fluid-wall interactions is the same for the A and B fluids. Thus, differences in the total free energy for the cases described below are solely due to the contribution of the A/B interfaces. The radius R of the droplets can be found by setting the area of each droplet equal to the initial area of one band [see Fig. 1(a)], hence

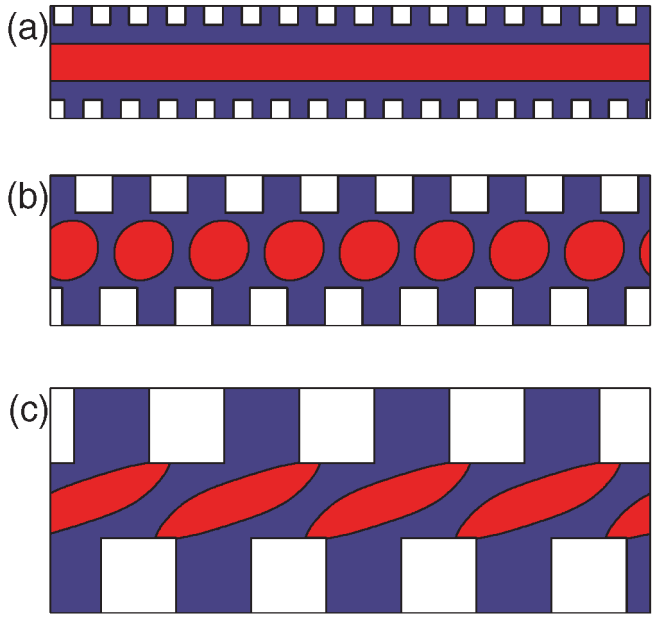

FIG. 2 (color online). Dynamic behavior of a regular array of bands, which bridge a narrow gap between square asperities on two parallel walls, for different ratios of the initial bandwidth W and the gap height H. The initial configuration was similar to that in Fig. 1(a). The system reached a final steady state for (a) $W/H = 1/4$ and (b) $W/H = 1/2$. For (c) $W/H = 1$, the system evolved to a state where bands break up and recombine in a periodic manner.

$R = \sqrt{WH/\pi}$. The droplet's interfacial length is then $2H\sqrt{\pi W/H}$, while the interfacial length of the bands is $2H$. Thus, for $W/H > 1/\pi$, it is energetically more favorable for the A fluid to form bands [4]. Consequently, when such bands are snapped off, there is an energetic driving force for them to reattach, causing the cycle to repeat itself (as is the case for $W/H = 1$ in Fig. 2(c)]. Similarly, by comparing the length of the appropriate horizontal segment, $(2G + 2H)$, with the circumference of the droplet, we find that it is energetically favorable to form a continuous, horizontal A band in the center of the gap when $(W + G)/H < \sqrt{\pi W/H}$ (as is the case for $W/H = 1/4$ and $G = W$ in Fig. 2(a)]. Note that the interfacial length of the center band grows with increasing G, whereas that of the droplet is independent of G. Therefore, coalescence can be prevented by placing the asperities sufficiently far apart, as can be seen by comparing Figs. 2(a) and 2(b). The above arguments are based on thermodynamics; however, the case of $W/H = 1/2$ and $G = W$ [see Fig. 2(b)] highlights the important interplay between thermodynamics and kinetics in controlling the structure of the system. It is actually energetically more favorable in this case to form either bands between the asperities or a single band in the center of the gap. Yet, once the droplets have been dynamically formed, the system stays trapped in a local free energy minimum because the energy barrier for the droplets to coalesce or reattach is too high.

To capture this complex behavior, we use a lattice Boltzmann model (LBM) for binary fluids [5]. This is a computationally efficient method for solving the coupled Navier-Stokes and convection-diffusion equations that describe the system. While this technique has been used to model mixtures under shear [6,7], this is the first extension of the method to sheared fluids that are confined between rough surfaces. In the LBM, the distribution functions $n^{(\alpha)}(\mathbf{r}, \mathbf{c}_i, t)$ describe the mass density of fluid particles of component α at a lattice node $\mathbf{r}$ with a velocity $\mathbf{c}_i$ at time t. The state of our system is characterized by the mass density distribution, $\rho_i(\mathbf{r}, t) \equiv n^{(1)}(\mathbf{r}, \mathbf{c}_i, t) + n^{(2)}(\mathbf{r}, \mathbf{c}_i, t)$, and the difference, $\phi_i(\mathbf{r}, t) \equiv n^{(1)}(\mathbf{r}, \mathbf{c}_i, t) - n^{(2)}(\mathbf{r}, \mathbf{c}_i, t)$. The "9-speed model," which includes the zero-velocity case (rest particles), is used to model the movement of particles along vectors that connect nearest and next-nearest neighbors on a square lattice. The conserved quantities, mass density $\rho(\mathbf{r}, t)$, momentum density $\mathbf{j}(\mathbf{r}, t)$, and order parameter $\phi(\mathbf{r}, t)$, are moments of the distribution functions; $\rho(\mathbf{r}, t) = \sum_i \rho_i(\mathbf{r}, t)$, $\mathbf{j}(\mathbf{r}, t) = \sum_i \mathbf{c}_i \rho_i(\mathbf{r}, t)$, and $\phi(\mathbf{r}, t) = \sum_i \phi_i(\mathbf{r}, t)$. Here, $\mathbf{j}(\mathbf{r}, t) = \rho(\mathbf{r}, t)\mathbf{u}(\mathbf{r}, t)$, and $\mathbf{u}(\mathbf{r}, t)$ is the macroscopic fluid velocity; the summations run over the discrete set of velocities $\{\mathbf{c}_i\}$.

The time evolutions of $\rho_i(\mathbf{r}, t)$ and $\phi_i(\mathbf{r}, t)$ are governed by the single relaxation-time lattice Boltzmann equations [8,9], $\rho_i(\mathbf{r} + \mathbf{c}_i, t + 1) = \rho_i(\mathbf{r}, t) - [\rho_i(\mathbf{r}, t) - \rho_i^{\mathrm{eq}}(\mathbf{r}, t)]/\tau_\rho$, and an equivalent one for $\phi_i(\mathbf{r}, t)$. Here, $\rho_i^{\mathrm{eq}}(\mathbf{r}, t)$ and

$\phi_i^{\rm eq}(\mathbf{r}, t)$ are the equilibrium distributions, which are constructed to conserve mass density, momentum density, and order parameter, and such that $\sum_i \mathbf{c}_i \mathbf{c}_i \rho_i^{\rm eq}(\mathbf{r}, t) = \mathbf{P} + \rho \mathbf{u}\mathbf{u}$, and $\sum_i \mathbf{c}_i \mathbf{c}_i \phi_i^{\rm eq}(\mathbf{r}, t) = \Gamma \Delta\mu \mathbf{1} + \phi \mathbf{u}\mathbf{u}$ [5]. Here, Γ is a coefficient related to the mobility, $M = \Gamma(2\tau_\phi - 1)/2$, and $\mathbf{P}$ and $\Delta\mu$ are the pressure tensor and the chemical potential difference between the two species, respectively. The latter quantities are obtained from the free energy functional, which is

$$F = \int d\mathbf{r} \left(\psi + \frac{\kappa}{2} |\nabla \phi|^2 \right), \tag{1}$$

with the free energy density defined as $\psi = \frac{1}{3}\rho \ln\rho - \frac{a}{2}\phi^2 + \frac{b}{4}\phi^4$ [10]. The term $\frac{1}{3}\rho \ln\rho$ does not affect the phase behavior, but is required in the LBM to enforce incompressibility to within acceptable numerical tolerances [10]. The remaining terms correspond to the usual Ginzburg-Landau free energy for a binary fluid (e.g., [11]). The parameters a, b, and κ determine the interfacial tension, $\sigma = \sqrt{8\kappa a^3/9b^2}$, and interface width, $\xi \approx 5\sqrt{\kappa/2a}$. While b and κ must be positive, a can be either negative (for a homogeneous state) or positive (for two coexisting phases). For our immiscible mixtures, $a = b > 0$, and the equilibrium values of the order parameters for two phases are $\phi_0 = \pm\sqrt{a/b} = \pm 1$.

In these simulations, the mean density $\langle\rho\rangle$ is set to unity and the ratio $\kappa/a = 0.64$, giving $\xi \approx 3$, which is the minimum acceptable value to obtain an accurately isotropic surface tension [10]. We selected $\tau_\phi = 1$, giving $M = \Gamma/2$, and then controlled the mobility through Γ. The remaining parameters were selected to ensure that the algorithm was stable, that inertial effects were small compared to viscous forces and surface tension, and that the diffusion was sufficiently rapid for the interfaces to relax to local equilibrium on a time scale that is fast compared to their translational motion. We used $\kappa = 0.04$, $\Gamma = 2$, and $\tau_\rho = 1$, giving $\eta = \rho(2\tau_\rho - 1)/6 = 1/6$; $H = 128$ in Fig. 2 and $H = 64$ in all other simulations. The relative velocity between both walls in Figs. 1 and 2 was 0.02.

The LBM must be modified to incorporate the no-slip boundary conditions imposed on the fluid by the solid phase. We used the link bounce-back method [12], in which the solid-fluid interface is represented by boundary nodes that lie midway between each solid and fluid node. It is straightforward to implement, even for arbitrarily complex surfaces, and gives stick boundary conditions for simple shear flow between planar interfaces.

Our mechanism for obtaining monodisperse droplets involves a special initial configuration, where bands of A are formed within the B phase and bridge the asperities. This configuration can be obtained by quenching an initially homogeneous mixture of the two components. Below the critical temperature, the homogeneous mixture is unstable against all fluctuations in the region where $\delta^2 F/\delta\phi^2 < 0$, with the free energy functional F defined in Eq. (1). Inside this so-called spinodal region, the mixed phase separates into domains where the order parameter takes on its equilibrium values $\pm\phi_0$. Outside the spinodal region, the system is metastable and a finite fluctuation or a nucleation site is needed to grow domains. Hence, there are basically two mechanisms to form bands through quenching. Which of these two applies depends on $\langle\phi\rangle$, the initial value of the order parameter in the homogeneous mixture. For a bulk mixture characterized by the free energy in Eq. (1), the border of the spinodal region is given by $\pm\phi_s$, with $\phi_s = \sqrt{a/3b}$ $(a, b > 0)$, while $\phi_0 = \sqrt{a/b}$. So for $|\langle\phi\rangle| < \phi_s$, the mixture undergoes spinodal decomposition, while for $\phi_s < |\langle\phi\rangle| < \phi_0$, this system exhibits nucleated growth.

For two arbitrary immiscible fluids, the formation of bands through spinodal decomposition is problematic since random fluctuations in the initial composition easily lead to a highly nonuniform morphology. However, the required uniform bands can be formed through nucleated growth by exploiting a selective wetting pattern at the walls [13]. In particular, small domains of a single component can be nucleated at specific wall areas by using patches that slightly favor only that component. Specific wetting conditions are accounted for by adding a surface free energy density ψ_s to F in Eq. (1) such that $F' = F + \int \psi_s dS$. Functional minimization of F' requires $\psi_s = \kappa\phi(\mathbf{n}\cdot\nabla\phi)$, evaluated at the wall, with $\mathbf{n}$ being the surface normal pointing into the fluid [14]. These wetting conditions are implemented in the LBM by enforcing a nonzero gradient of the order parameter at the walls. The static contact angle at the wall in the absence of flow is then $\cos\theta = \frac{1}{2}[(1+h)^{3/2} - (1-h)^{3/2}]$, with $h = (\mathbf{n}\cdot\nabla\phi)\sqrt{2\kappa/a}$.

The nucleation process is illustrated in Fig. 3 for a system having a geometry similar to that in Fig. 1. The tops of the asperities slightly favor one component, just

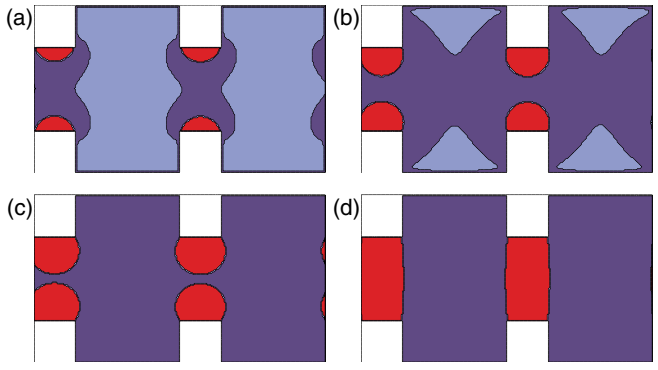

FIG. 3 (color online). Formation of bands through nucleated growth from an initially homogeneous mixture (light gray). The tops of the asperities slightly favor one component (gray), while the pockets selectively wet the other component (dark gray).

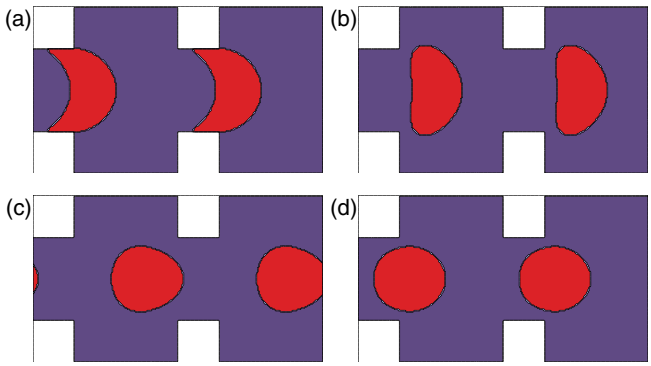

FIG. 4 (color online). Formation of droplets from a regular array of bands under pressure driven flow. The initial configuration is identical to that of Fig. 3(d), the applied pressure gradient is 2×10^{-5}

enough to initiate nucleation, while the pockets between the asperities selectively wet the second component. This particular geometry and wetting pattern can readily be fabricated through standard microcontact printing methods [15]. The initial value of the order parameter is chosen such that (i) it lies inside the nucleation region, and (ii) there is enough of the minority component to form bands that bridge the gap between the asperities. Bands of equal volume are then formed if the mixture before quenching is sufficiently uniform and if the asperities are placed equal distances apart.

While absent in two dimensions, the Rayleigh instability can cause planar sheets and cylindrical domains to break up into droplets in three dimensions. The same instability can cause droplets once formed to break up into smaller ones under the influence of a shear flow [16]. This breakup process is controlled by the capillary number, $\mathrm{Ca} \equiv \eta\dot{\gamma}R/\sigma$, characterizing the relative importance of shear stress and surface tension. Here, η is the viscosity of the B phase, $\dot{\gamma}$ is the applied shear rate, σ is the surface tension, and R is the radius of the A droplets. Hence, in experiments and in three-dimensional simulations, Ca must be $\ll 1$ to ensure the formation of stable droplets.

The most relevant dimensionless numbers that characterize the shear flow are the capillary number, as defined above, and the Reynolds number, based on the shear rate and droplet radius, $\mathrm{Re} \equiv \rho\dot{\gamma}R^2/\eta$. For a typical binary fluid, $\sigma = 0.01\ \mathrm{Nm}^{-1}$, $\eta = 0.05\ \mathrm{Pa\,s}$, and $\rho = 1000\ \mathrm{kg\,m}^{-3}$. Hence, $R = \mathrm{Re}/400$ for $\mathrm{Ca} = 0.1$. For stability reasons, the maximum wall velocity in the LBM units is about 0.1, while the range of viscosities is from 0.01 up to about 10. Thus, for a typical simulation with $R = 64$, $H = 128$, $\mathrm{Ca} = 0.1$, and the same free energy parameters as used above ($\kappa = 0.04$, $\kappa/a = 0.64$, and $a = b$), we can simulate a range of Reynolds numbers between 0.003 and 30. This corresponds to droplets with a radius between 7.5 μm and 75 mm. The corresponding values of W and G would also be of the same order.

Although droplet formation in a shear cell is experimentally quite feasible, it might be preferable to have a fixed geometry and form droplets by applying a pressure gradient along the gap. We can tune the pressure gradient such that the bands snap off at the wall, without compromising the integrity of the band itself. Hence, under the correct conditions, as illustrated in Fig. 4, droplets can just as readily be obtained through an imposed pressure gradient as through a steady shear.

In three dimensions, the appropriate confining walls would contain regularly spaced cubic or cylindrical asperities [17]. Such surfaces can be fabricated in the micron to mm range [15], thus permitting significant control over the size scale of the droplets. This has important technological implications for creating well-defined emulsions. On a more fundamental level, these findings uncover a rich phase behavior that emerges when multicomponent fluids are driven to flow over surfaces that contain both chemical and physical heterogeneities. These studies are vital to enhancing our understanding of such disparate processes as blood flow in arteries to polymer processing in reaction chambers.

The authors gratefully acknowledge helpful conversations with Dr. D. Marenduzzo and Professor A. J. C. Ladd. This work was supported by the Office of Naval Research.

[1] O. Kuksenok, D. Jasnow, and A. C. Balazs, Phys. Rev. E **68**, 051505 (2003), and references therein.
[2] P. B. Umbanhowar, V. Prasad, and D. A. Weitz, Langmuir **16**, 347 (2000), and references therein.
[3] T. Thorsen, R. W. Roberts, F. H. Arnold, and S. R. Quake, Phys. Rev. Lett. **86**, 4163 (2001).
[4] If the asperities favor the A phase, the critical ratio will be higher, but the qualitative picture remains the same.
[5] M. R. Swift, E. Orlandini, W. R. Osborn, and J. M. Yeomans, Phys. Rev. E **54**, 5041 (1996).
[6] A. J. Wagner and J. M. Yeomans, Phys. Rev. E **59**, 4366 (1999).
[7] A. Xu, G. Gonnella, and A. Lamura, Phys. Rev. E **67**, 056105 (2003).
[8] S. D. Chen, H. D. Chen, D. Martinez, and W. Matthaeus, Phys. Rev. Lett. **67**, 3776 (1991).
[9] Y. H. Qian, D. d'Humières, and P. Lallemand, Europhys. Lett. **17**, 479 (1992).
[10] V. M. Kendon, M. E. Cates, I. Pagonabarraga, J.-C. Desplat, and P. Bladon, J. Fluid Mech. **440**, 147 (2001).
[11] A. J. Bray, Adv. Phys. **43**, 357 (1994).
[12] A. J. C. Ladd, J. Fluid Mech. **271**, 285 (1994).
[13] Here, "nucleated growth" means that wall interactions drive the fluid into the spinodal region.
[14] J. W. Cahn, J. Chem. Phys. **66**, 3667 (1976).
[15] A. Kumar, H. A. Biebuyck, and G. M. Whitesides, Langmuir **10**, 1498 (1994).
[16] A. J. Wagner, L. M. Wilson, and M. E. Cates, Phys. Rev. E **68**, 045301 (2003), and references therein.
[17] Preliminary findings from 3D simulations show behavior that is qualitatively similar to Fig. 2.